An Investigation of Systematic Errors in the Barotropic Forecasts[1]

By Lt. Col. DONALD E. MARTIN, USAF, International Meteorological Institute in Stockholm

(Original manuscript received April 1. 1958; revised July 30, 1958)

Abstract

Forecast-errors in the 24- and 48-hour barotropic 500-mb prognostic charts prepared by JNWPU for the winter of 1957 were investigated. Certain large-scale forecast-errors were found to persist from day-to-day in fairly localized geographical areas. In general, the numerical prognoses exhibited a tendency to forecast excessively high values off the southeastern coasts and excessively low values off the northwestern coasts of the continents. Little forecast-error was observed in the continental interiors.

A Fourier analysis revealed that the forecast-errors were largely due to incorrect phase forecasts for wave numbers 1 through 4.

The forecast-errors associated with wave number 1 usually "positioned" the large-scale systematic forecast-errors near Japan and Scandinavia and contributed materially to their intensities.

Relationships between forecast-error fields and topography, geography, synoptic situation, and "non-adiabatic" heating are discussed.

Hemispheric fields of "non-adiabatic" heating, computed using a two-level graphical model, are shown.

Charts illustrating the dependence of "non-adiabatic" heating on the general circulation are also shown.

I. Introduction

The Joint Numerical Weather Prediction Unit of the United States has been issuing hemispheric 500-mb prognostic charts for an octagonally-shaped area, centered on the North Pole and extending down to approximately 13° N latitude, since October 1957. The model used differs from other barotropic models in the following respects:

a. A mountain effect has been incorporated by introducing the vertical velocity at the earth surface, produced by a flow over the terrain, into the potential vorticity equation.

b. A non-divergent wind is employed by solving the balance equation.

c. A smoothing operator is used every twelve hours to eliminate fluctuations with wavelengths of about 700 kilometers or less while longer wavelengths are left practically intact.

d. The stream function and the relative vorticity are held fixed on the boundaries.

The skill that the barotropic forecast model exhibits in forecasting atmospheric changes is readily obtained by studying the errors in the forecasts. Since the numerical prognoses are objective and mathematically-produced, the systematic forecast-errors should reveal those instances where the model is least efficient in its representation of true atmospheric motions.

With the hope that the barotropic forecasts would offer a deeper insight into the problems of numerical forecasting, and afford a base from

[1] Part of the research reported in this document has been sponsored by the U.S. Weather Bureau under contract No. Cwb-9316.

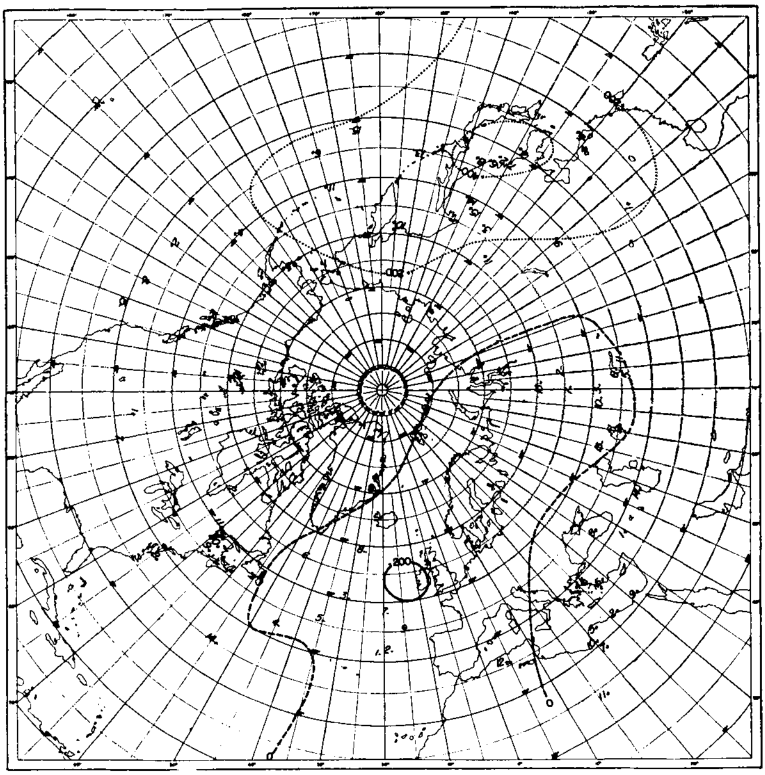

Fig. 1. Large scale 48-hour forecast errors for November 1—15, 1957. The isolines are drawn for averaged values of 500-mb space-meaned 48-hour prognostic minus space-meaned observed analysis. Each number followed by a plus or minus sign marks the position, date, and sign of a daily 48-hour space-mean forecast-error center which exceeded 200 feet.

which improvements could be effected, the prognosis were investigated to determine:

a. The spatial distribution of the large-scale forecast-errors.

b. The relationship between the error fields and the earth's topography, the synoptic situation, and the geographical location.

c. The effects that the assumptions inherent in a barotropic forecast model have on disturbances of different amplitudes and wavelengths during progressively longer time intervals.

The diagnostic aspect of this investigation will be presented at this time. The results of experiments designed to improve these prognoses will be published in a later report.

II. Data used

The JNWPU 24-, 48-, and 72-hour prognostic charts and the verifying observed analysis for the period 1 October 1957 to 1 February 1958 were used in connection with sections III and IV. NWAC's twice-daily hemispheric sea-level analysis and the JNWPU 500-mb analysis for the period 15—31 December 1957 were used in section V.

Three non-consecutive, half-monthly periods for which a complete series of maps were available were used to compile the statistics in section IV. The periods were November 1—15, 1957, December 15—31, 1957, and January 15—31, 1958. This choice was made in an effort to minimize the possibility that the same synoptic situation would persist throughout all of the statistical data.

III. The spatial distribution of the large-scale forecast-errors

The prognostic charts and the observed analysis were graphically space-meaned to smooth out the small scale fields, thereby delineating the large-scale ones. The distance increment used was equal to 11.2 deg. of latitude on the map at 45 deg. N. The 24- and 48-hour observed and forecast height changes in these space-mean charts, and the corresponding error

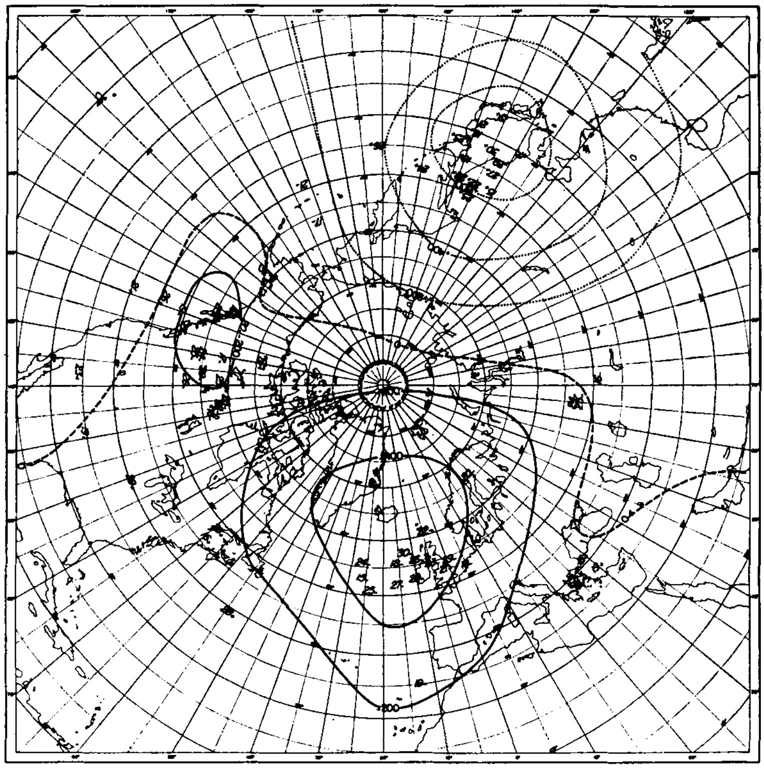

Fig. 2. Large scale 48-hour forecast errors for December 15—30, 1957 (refer to Fig. 1 for further explanation).

fields on the space-mean of the prognostic charts, were similarly computed.

In the discussion to follow in section III, unless otherwise stated, the expression "error field" will refer to forecast errors on the space-meaned prognostic charts; i.e., space-meaned prognostic chart minus space-meaned observed analysis. Similarly, the term "changes" will refer to changes in the space-mean charts.

Since a forecast error can result from numerous effects, any discussion of the possible association between error fields and other phenomena will refer only to some undetermined fractional portion of the error field in question. In other words, no attempt will be made to explain all of the errors, or to compare errors due to analysis, computation, data transmission, etc. with those caused by terrain, season, geographical location, or synoptic event.

The following indications were evident on this series of space-mean-charts:

a. Forecast-errors of sufficient magnitude to appear on the space-mean chart exist.

b. The magnitude of the forecast-errors usually exceeded the magnitude of the observed changes over a forecast period. (This does not imply, however, that the error centers and the change centers are necessarily related.)

c. The magnitude of the error fields increased as the forecast period increased and as the season progressed from October through January.

d. Any logical day-to-day continuity of motion of either the *transient* forecast-error centers or observed change centers was very difficult to establish.

e. The forecasts for the regions from the Asiatic Coast to the Mid-Pacific and from the central Atlantic to Scandinavia exhibited a tendency throughout the data for positive and negative errors, respectively.

Examples are given for the periods Nov. 1—15, 1957, Dec. 15—30, 1957 and Jan. 15—30, 1958 in figures 1, 2 and 3, respectively, to substantiate the above statements. Each illustration was constructed in the following manner:

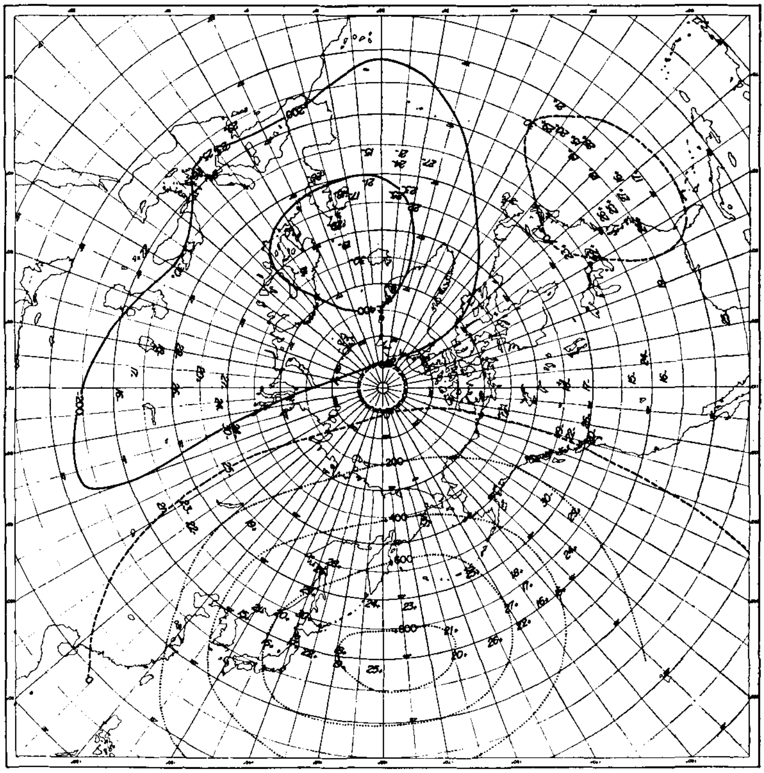

Fig. 3. Large scale 48-hour forecast errors for January 15—30, 1958 (refer to Fig. 1 for further explanation).

a. Each of the 16 consecutive 0000Z, 500 mb observed analyses was space-meaned.

b. These 16 space-meaned charts were then graphically averaged.*

c. A similar space-meaning and averaging procedure was applied to the 48-hour prognoses valid on the same 16 days.

d. The mean error field for the 16-day period was derived by graphical subtraction of the averaged analysis and prognostic fields.

e. The positions of all error centers (greater than 200 feet) which were observed on each of the 16 days (they were computed by graphical subtraction of the space-meaned analysis and prognostic charts for each day) are entered by the date and algebraic sign of the error.

A positive mean-error center near the Asiatic Coast and a negative one near Europe are common to all three figures. In fact, errors in these regions were sufficiently persistent to predominate over other more transient error fields in every investigation in this project. The tendency for the daily forecast-error centers to cluster in these areas during December can be seen in figure 2.

During the entire 4-month period of data from November 1957 through February 1958 not more than one or two daily 48-hr negative forecast-error centers appeared over the Pacific region near Japan. Similarly, very few positive error centers were found over the Northeastern Atlantic. This seems to imply that these errors are systematic and are either geographically dependent or result from the model's mistreatment of those persistent waves which are, in turn, geographically dependent. Thus, it appears that the effects of terrain and of heat sources and sinks warrant further investigation. However, of equal importance, is the model's persistent tendency to drastically retrograde the very long waves (>90 deg. longi-

* Such a procedure, i.e. taking an average of 16 space-mean charts, should minimize all but the most intense or persistent daily forecast-error fields. Sixteen maps were chosen (in preference to 15) to simplify the graphical computations. (See IWW special study 105-2, app. II P. 124).

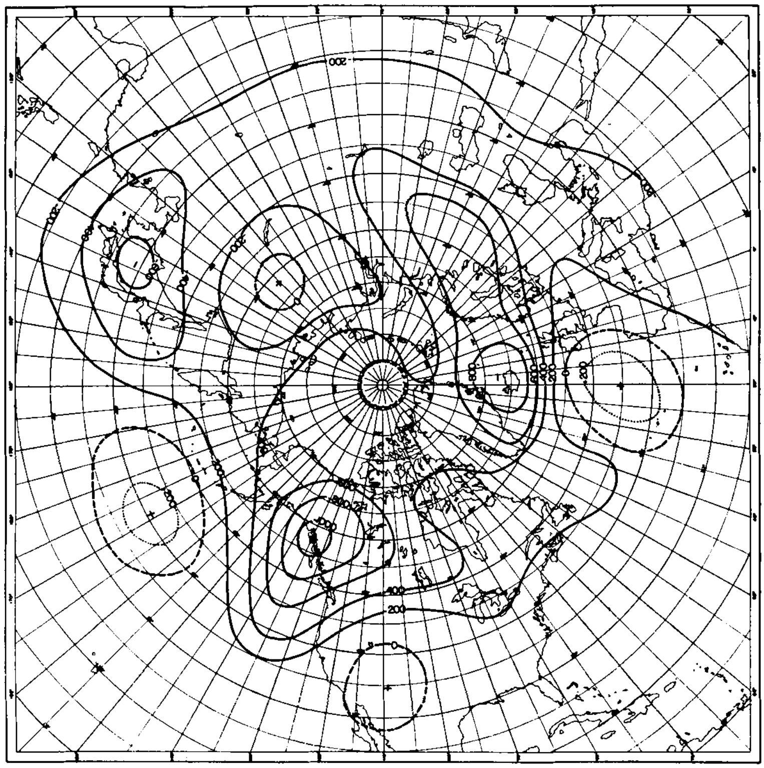

Fig. 4. The averaged-observed 500-mb contour-difference between the periods November 1—15, 1957, and December 15—30, 1957.

tude); this similarly warrants consideration. (see section IV). These observations and the experiments in progress at the Institute of Meteorology in Stockholm to investigate their causes will be discussed throughout this report.

An attempt to follow the continuity of the daily positions of the transient-error centers in either figure 1, 2 or 3, would show the difficulty to be encountered in trying to forecast changes in the large-scale error fields. A comparison of figures 1 and 2 reveals that larger mean-errors were observed in December than in November. Also, the daily centers were more transitory in November. Whether this latter observation is associated with the more changeable circulation patterns of November is problematical. Of more significance, perhaps, is an apparent tendency for the daily error centers to "cluster" in Northwest Canada in December. The difference between the averaged observed circulation patterns for December and November is shown in figure 4 to illustrate the relationship between changes in the error fields and changes in the circulation patterns.

A comparison of figure 4 with figures 1 and 2 over Northwest Canada implies that a relationship does exist between changes in the mean-error fields and changes in the circulation pattern. However, the relationship is not uniquely established by such a comparison. For instance, the negative circulation-pattern change center located over Japan in figure 4 is associated with larger *positive* mean-errors in December than in November. Again, caution must also be exerted in drawing conclusions from the latter comparison. For instance, there is no proof that the forecast-errors in Japan and Northwest Canada are related; i.e., one may be related to a topographical condition and the other to a synoptic event. (This possibility will be discussed further in section IV. There it will be seen that the errors over Canada for this period are primarily associated with 90 degree wavelength features and the errors over Japan with 360 degree wavelengths).

Figure 3 reveals larger forecast mean-errors than those in either figure 1 or 2. Two other major differences are also found. The positive mean-error center in the Pacific is located further east in January and a positive mean-error center is found over the south-eastern United States which was not apparent in November or December. Undoubtedly, some of the difference between forecast-errors on figures 1 or 2 and those on figure 3 in the Pacific is attributable to a lack of data. However, factors such as stronger wind patterns and increased temperature gradients between the Asiatic continent and the ocean could also presumably contribute to the eastwardly displaced and more intense mean-errors in January

SIGTRYGGSSON and WIIN-NIELSEN (1957), in an investigation of non-adiabatic effects for the Western hemisphere, found heat-source and heat-sink patterns resembling the mean-error field over the United States in figure 3. MARTIN (1956), in a similar investigation for the Eastern hemisphere, found a source-and-sink pattern resembling the Pacific portion of the mean-error field in figure 3.

A detailed discussion of some "non-adiabatic effects" will be given in section V.

IV. A Fourier analysis of the numerical prognostic charts

A Fourier analysis was made of the numerical forecasts and the verifying observed analyses for the three previously-mentioned half-monthly periods. The computations were made using an I.B.M. code which required data from 100 points along the 45° N latitude circle. Amplitudes were obtained for the first fifteen sine and cosine components based on the equation

$$z(x) = \frac{a_0}{2} + \sum_{K=1}^{15} a_K \cos Kx + b_K \sin Kx)$$

In the above formula $z\ (x)$ is the 500 mb height at position X on the 45° N latitude circle, $\frac{a_0}{2}$ is the average 500 mb height around the same circle, K is the wave number, and X the longitude. X is zero at 0° longitude and the positive direction is oriented to the east.

The coefficients a_K and b_K were used to compute the amplitude A_K and the phase angle ϕ based on the formula

$$z(x) = \frac{a_0}{2} + \sum_{K=1}^{15} A_K \cos\ (Kx - \phi)$$

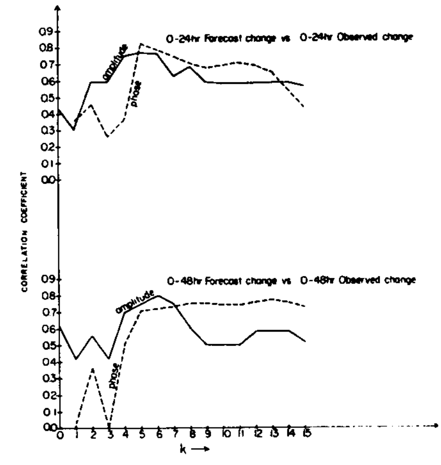

Fig. 5. Coefficients of correlation between forecast and observed changes in amplitude and phase for wave-numbers 1 through 15. The correlations are based on 47 pairs of data obtained from the periods, November 1—15, 1957, December 15—30, 1957, and January 15—31, 1958.

The relationship between the two formulae is given by $A_K = \sqrt{a_K^2 + b_K^2}$ and $\phi = \cot^{-1} \frac{a_K}{b_K}$. A graph devised by HARRIS (1956) was used to convert the machine data to this new form.

Coefficients of correlation between the forecast and observed changes in amplitude and phase angle for the 24- and 48-hour period are shown in figure 5. These coefficients are based on 47 pairs of data (15 for November, 1957, 16 for December, 1957, and 16 for January, 1958). The graphs indicate that, in general, larger correlation coefficients are found for wave numbers 5 and higher than for wave numbers 4 and lower. This figure further indicates that, for long waves (small wave numbers), the barotropic model forecasts amplitude changes better than phase changes. For the shorter waves, the situation is essentially reversed; i.e., phase changes are forecast more accurately than amplitude changes.

The amplitude and phase forecasts for certain wave components showed a rather consistent daily-forecast error. Some of these will be cited at this time. During the 24-hour period, a forecast for an increase in the average height about the 45° N latitude circle was made 90 % of the time; however, observed height increases occurred only 26 % of the time. This small percentage of observed occurrence was probably due to the progression of the data toward the colder season where the average heights are characteristically less than in the warmer season. The average forecast-error was approximately + 70 feet for the first 24 hours. For the 48-hour period, the average height was forecast to increase 81 % of the time and positive changes verified 30 % of the time. An average forecast-error of approximately + 100 feet in 48 hours was observed.

Westward phase-displacements in wave number 1 were forecast 92 % of the time for the 24-hour period and such changes were verified 50 % of the time. The average 24-hour phase error was −40 deg. of longitude. For the 48-hour period, the forecast westward phase-displacement was sufficiently large to bring about an almost complete reversal of phase. In reality, the observed amplitude and phase values for this wave-components were very persistent. The out-of-phase relationship which resulted between the forecast and observed values gave forecast-errors at the "troughs" and "ridges", which were almost twice the magnitude of the observed amplitudes of wave number 1.

The amplitudes of wave number 1 were forecast to decrease 91 % of the time and observed to decrease 66 % of the time during the 24-hour period. An average error of − 110 feet was found. For the 48-hour period, decreasing amplitudes in wave number 1 were forecast 94 % of the time and observed 64 % of the time. The average error was − 220 feet.

Wave number 2 exhibited no recognizable tendency for a forecast-bias in amplitude changes for either 24 or 48 hours. However, a westward phase-displacement was forecast 92 % of the time and observed 55 % of the time for 24 hours. For the 48-hour period, a westward phase-displacement was forecast 77 % of the time and observed 65 % of the time. The average forecast error was −19° longitude for 24 hours and −24° longitude for 48 hours.

Similarly, the forecast *amplitude* changes in wave number 3 displayed little, if any, bias for either the 24- or 48-hour period. However, westward phase-displacements were forecast 83 % of the time on the 24-hour prognoses and 85 % of the time on the 48-hour ones. Such displacements occurred 64 % and 60 % of the time respectively. The average forecast error was −6° longitude in 24 hours and −20° longitude in 48 hours.

The forecasts of wave number 4 for 48 hours showed an average error of − 50 feet in amplitude and an error of about −4° longitude in phase. Westward phase-displacements in 48 hours were forecast 50 % of the time versus 25 % observed. A similar ratio was found for the 24 hour forecasts.

No consistent bias in the phase forecast for shorter wavelengths was evidenced. However, the forecasts for wave numbers 5, 6, 7 and 8 exhibited a tendency to diminish the amplitude by an average of 50 feet or so in 48 hours.

In an attempt to portray the foregoing discussion more pictorially, mean-Fourier components were computed using the 16 daily components for each of the three periods – November 1—15, 1957, December 15—31, 1957, and January 15—31, 1958. The mean-Fourier Components for wave numbers 1 through 6 for the observed, 24-, and 48-hour components during the December period are shown in figure 6. The December components are presented here, rather than the November or January ones, since the data for December has been more thoroughly investigated in conjunction with heat sources and sinks than the other periods. This latter aspect will be discussed in section V.

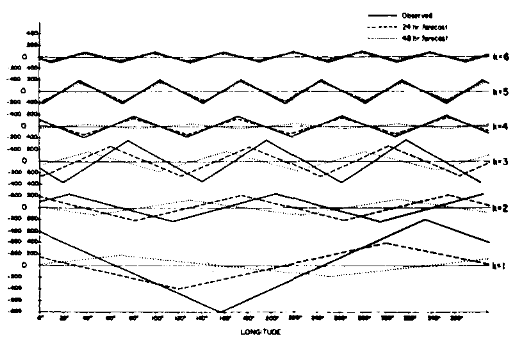

Fig. 6. Mean-Fourier components of observed, 24-, and 48-hour forecasts for December 15—31, 1957. The ordinate represents amplitude in feet. The abscissa denotes longitude. Increasing longitude values are oriented toward the east.

The sine waves have been replaced by triangles, in figure 6, so that the exact location of troughs and ridges can be seen more readily. This was deemed advisable since the main discussion of the figure will pertain to the relationship between observed and forecast phase angles.

In reference to wave number 1 in figure 6, errors in 24 hours are seen to arise from the forecast tendency to retrograde the wave and diminish its amplitude. For the 48-hour period, the forecast is almost completely out of phase. As previously mentioned, this is evident from the statistics of the individual cases comprising the mean as well. Such forecast-errors in wave number 1, alone, were found to account for a sizeable portion of the error fields shown in figures 1, 2, and 3.

Figure 6 also shows the general tendency for a forecast retrogression of wave numbers 2 and 3, while wave number 4 shows an almost complete reversal of phase. The same type of error in the forecasts for wave numbers 1, 2 and 3 as those seen in figure 6 were also found in November and January. However, the forecast errors in wave number 4 are *not* characteristic of the November and January periods. In these latter-mentioned periods, the forecasts for wave number 4 were much better.

Agreement between 24- and 48-hour forecasts and observed values in wave numbers 5 and 6, comparable to that seen in figure 6, is common to all three periods. Similar agreement was found for wave numbers 7 and 8. No attempt was made to extend the analysis to higher wave numbers since the mean-Fourier amplitudes become negligibly small for higher wave numbers.

Graphs showing the distribution of the geostrophic meridional-component of kinetic energy for wave components 1 through 15 are shown in figure 7. These graphs were obtained using the formula

$$Ke_K = \frac{2g}{L}\left(\frac{\pi}{f}\right)^2 \int\limits_{P}^{P+\Delta P} \int\limits_{y}^{y+\Delta y} (a_K^2 + b_K^2)\, K^2\, dy dp$$

for each of the three half-monthly periods. In this formula, Ke_K is the kinetic energy for a particular wave number, K. L is the length of the latitude circle, and f the coriolis parameter.

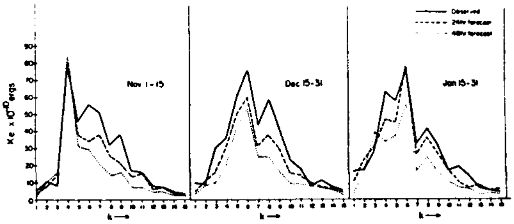

Fig. 7. Average values of kinetic energy of north-south motion for wave number $k = 1, 2, \ldots 15$, for November 1—15, 1957, December 15—31, 1957, and January 15—31, 1958.

In all computations, a ring of unit pressure-difference in the vertical and of unit latitudinal extent was considered. A more detailed discussion of the computational method is found in a paper by WHITE and COOLEY (1956).

Generally speaking all the waves underwent a loss of meridional kinetic energy in the forecast. The greater loss was suffered by the shorter waves (higher wave numbers). Since the smoothing operator used in making the numerical forecasts had little effect on any of these first fifteen wave components, it appears that causes other than smoothing were responsible for this energy loss.

In order to establish more accurately how this loss of energy occurred, the *total* kinetic energy for each wave component is needed. Since a barotropic forecast over a closed region conserves the total initial energy, an analysis of the total kinetic energy spectrum should reveal whether or not the meridional kinetic energy loss, in the first fifteen components, is associated with energy gains in other portions of the wave spectrum. If a loss of total kinetic energy is actually being forecast, such factors as incorrect boundary conditions, smoothing, and errors resulting from finite-difference approximations need further considerations.

Certain error fields were discussed in section III in conjunction with the large-scale circulation. A continuation of that discussion will be given here. Assuming that the sum of the average height and wave components 1 through 4 depict the long wave profile, the daily data for each of the periods, November 1—15, 1957, December 15—31, 1957, and January 15—31, 1958 were used to obtain half-monthly mean long wave profiles for the observed, 24-,

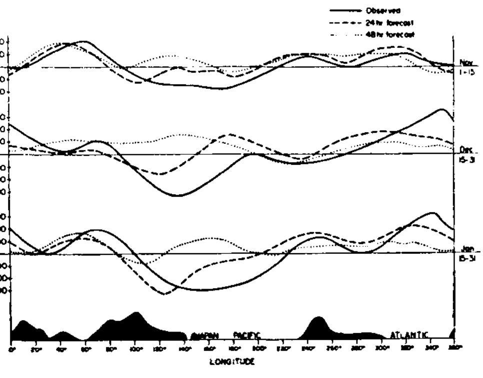

Fig. 8. Observed, 24-, and 48-hour 500-mb forecast long wave profiles at 45° N for November 1—15, 1957, December 15—31, 1957, and January 15—31, 1958. The ordinate represents the difference in feet between the sum of the average height and components 1 through 4 and the observed longitudinally-averaged 500-mb height for the same period.

and 48-hour forecasts. These profiles are shown in figure 8. Note the difference in the profiles over Northwest Canada between November and December. Much of this difference is due to wave component number 4. A crest in wave number 4 was quite persistent near 230 deg. (Gulf of Alaska) in November, and an equally persistent "trough" in wave number 4, was found in that same general vicinity in December from an inspection of the daily Fourier-components. The daily observed 500-mb charts for these periods also verify the persistence of a long wave 500-mb contour ridge in November and trough in December in the Gulf of Alaska. Apparently, some of the cyclonic vorticity advected out of the long wave troughs during December was not conserved thereby contributing to generally lower forecast values of the 500-mb surface than those observed.

So far we have shown the dependence of certain forecast-error fields on geographic location. We have also observed that large negative forecast-errors are frequently found along the northwestern coasts, large positive errors along the southeastern coasts, and relatively small forecast-errors over the interiors of Asia and North America. Furthermore, the more systematic forecast-errors were observed to result from a rather consistent forecast tendency to retrograde the quasi-stationary long waves.

These observations give rise to the following pertinent questions. Do the forecast-errors result primarily from certain deficiencies in the model which do not account for those factors which maintain the more or less forced oscillations in various preferred geographical locations; or, are the errors primarily due to incorrect forecasts of certain synoptic events (cyclogenesis, anticyclogenesis, etc.) which favor specific geographical locations for their development?

In order to investigate the dependence of the daily forecast-errors in wave number 1 on the observed trough location, the daily 24- and 48-hour phase errors were plotted as a function of the initial observed longitude of the "trough" in wave number 1. This investigation used the 47 days of statistical data previously considered in the correlation study.

It was found that the observed trough in wave number 1 was located in all cases somewhere in the interval between 140° East and 157° West longitude. A plot of phase-errors in the daily 24- and 48-hour forecasts versus the observed daily trough-locations showed *no* recognizable dependence of the phase-errors on the position of the observed trough at forecast time (i.e. essentially the same error was made for troughs located in the Central Pacific as for those located near the Asiatic coast).

In view of the material presented so far, several factors appear worthy of further consideration. An improvement in the operational forecasts can be effected by simply forecasting the long waves to persist during the forecast period. A procedure based on such reasoning has been inaugurated by JNWPU, see WOLFF (1958).

At best, however, this should be only a "stop gap" measure. It eliminates all hope of issuing numerical long range forecasts since it considers the very thing we want to forecast as being invariant.

The systematic tendency to forecast the very long waves to retrograde suggests that a deficiency in the model might arise from an incorrect assessment of that mechanism which causes these waves to remain quasi-stationary. One possibility is that vertically-averaged divergence fields in nature are counteracting the forecast retrogressive tendency for these long waves. Such fields would exert less influence on the motion of shorter waves than on the longer ones as readily seen from the various frequency equations for the speed of long waves. The accuracy with which the motion of the short waves is being forecast in comparison with the longer waves is in agreement with the type of results attributable to the neglect of divergence in the model. A hemispheric code is being prepared for BESK to test models which incorporate the divergence term, see BOLIN (1955).

Presently, hemispheric time-averaged fields of divergence are being computed for the winter months using the vertical velocities associated with both adiabatic and non-adiabatic heating and cooling (see section V).

It is hoped that the divergence fields can be calculated with sufficient accuracy to determine the role that these fields might play in maintaining the quasi-stationary long wave troughs off the Japanese and North American coasts.

V. Non-adiabatic effects

A somewhat simplified model for calculating "non-adiabatic" heating has been devised. This model is similar to other two-layer models conventionally used in numerical forecasting. Graphical procedures have been used to compute the combined "non-adiabatic" heating arising from sources other than friction. In this investigation, all the errors in the forecast are assumed to result from heating and cooling. In the model, the wind is assumed to vary linearly with height, the vertical advection of vorticity and the twisting terms are neglected, the relative vorticity is considered small in comparison with the coriolis parameter in the divergence term, the static stability is considered invariant, and the effects of friction are neglected.

The vorticity equation in the form

$$\frac{\partial \zeta}{\partial t} + \mathbf{v} \cdot \nabla \eta = f \frac{\partial \omega}{\partial P} \qquad (1)$$

has been used where ζ is the relative vorticity, η the absolute vorticity, f the coriolis parameter, and where ω is $\frac{dp}{dt}$.

In order to apply finite difference aproximations, the atmosphere is divided into layers as follows:

a	0 mb
b	250 mb
c	500 mb
d	750 mb
e	1000 mb

The term, $\frac{\partial \omega}{\partial p}$ in equation 1 is evaluated using finite differences between levels c and e while applying the vorticity equation at level d.

$$\left(\frac{\partial \zeta}{\partial t} + \mathbf{v} \cdot \nabla \eta\right)_d = \frac{f}{P^\star} (\omega_e - \omega_c) \qquad (2)$$

where $P^\star$ refers to a pressure difference of 500 mb. Solving for ω_c gives

$$\omega_c = -\frac{P^\star}{f} \left(\frac{\partial \zeta}{\partial t} + \mathbf{v} \cdot \nabla \eta\right)_d + \omega_e \qquad (3)$$

Another expression containing ω_c is obtained from the thermodynamic energy equation

$$\frac{dQ}{dt} = C_P \frac{dT}{dt} - \alpha \frac{dp}{dt} \qquad (4)$$

Here T = temperature, P = pressure, α = specific volume, t = time, and $\frac{dQ}{dt}$ the amount of non-adiabatic heating.

By the use of Poisson's equation, the equation of state and hydrostatic relationships, equation 4 is converted to the form

$$-\frac{R}{C_P p} \frac{dQ}{dt} = g \left[\frac{\partial}{\partial t}\left(\frac{\partial z}{\partial p}\right) + \mathbf{v}_2 \cdot \nabla \left(\frac{\partial z}{\partial p}\right)\right] + \omega\sigma \qquad (5)$$

where $\mathbf{v}_2$ refers to the horizontal wind on a constant pressure surface and $\sigma = -\alpha \frac{\partial}{\partial p} \ln \Theta$. The symbol Θ denotes potential temperature. A "vertically averaged" value for $\frac{dQ}{dt}$ is obtained by applying equation (5) to the 500-mb level.

$$-\left(\frac{-R}{C_P P} \frac{dQ}{dt}\right)_c = -\frac{g}{P^\star} \left(\frac{\partial h}{\partial t} + \mathbf{v}_c \cdot \nabla h\right) + (\omega\sigma)_c \qquad (6)$$

The thickness, h, actually pertains between levels b and d. However, the assumption of a linear wind distribution with height permits substitution of the thickness between 1000 and 500-mb in the advective term of (6). Substituting from (3) for ω_c in (6) gives

$$\left(\frac{R}{C_P P}\frac{dQ}{dt}\right)_c = \frac{g}{P^\star}\left(\frac{\partial h}{\partial t} + \mathbf{v}_c \cdot \nabla h\right) + + \frac{P^\star}{f}\sigma_c\left(\frac{\partial \varepsilon}{\partial t} + \mathbf{v}\cdot\nabla\eta\right)_c - \sigma_c\omega_c \tag{7}$$

multiplying (7) by $\frac{P^\star}{2g}$ yields, since $P^\star = P_c = = 500$ mb,

$$\frac{R}{2C_P P}\left(\frac{dQ}{dt}\right)_c = \frac{1}{2}\left(\frac{\partial h}{dt} + \mathbf{v}_c\cdot\nabla h\right) + + \frac{P^{\star 2}\sigma_c}{2gf}\left(\frac{\partial\varepsilon}{dt} + \mathbf{v}\cdot\nabla\eta\right)_d - \frac{\sigma_c\omega_e P^\star}{2g} \tag{8}$$

Substituting the expressions

$$(\varepsilon_g)_d = -\frac{4gm^2}{fd^2}(z - \bar{z})_d$$

and

$$(\eta_g)_d = -\frac{4gm^2}{fd^2}(z - \bar{z} - G)_d$$

in the second term on the right of (8) gives

$$\frac{R}{2C_P g}\left(\frac{dQ}{dt}\right)_c = \frac{1}{2}\left(\frac{\partial h}{\partial t} + \mathbf{v}_c\cdot\nabla h\right) - - \frac{2P^{\star 2}\sigma_c m^2}{f^2 d^2}\left(\frac{\partial}{\partial t}(z - \bar{z}) + \mathbf{v}\cdot\nabla\,(z - \bar{z} - G)\right)_d - - \frac{P^\star}{2g}\sigma_c\omega_c. \tag{9}$$

G is dependent on latitude only and accounts for the earth's vorticity, see Fjørtoft (1952). Its field can be charted once and for all for specific map projections. The letter, m, refers to the map projection and is assumed equal to 1. A distance of approximately 1000 kilometers is used for d, the increment of space smoothing. σ_c was determined at 45° N from the standard atmosphere. A numerical value of approximately 2 in the meter-ton-second system was found. A value of 10^{-4} was used for f in the calculation of the coefficient in (9) (but not in the G field). Using these values, the coefficient of the center term on the right hand side in (9) acquires an absolute value of 1.

The value of the term $\mathbf{v}_c \cdot \frac{\nabla h}{2}$ in (9) is equal to $\mathbf{v}_{750}\cdot\nabla\frac{h}{2}$ under the assumption of a linear wind field with height. Combining the first two terms on the right in (9) and substituting $\omega_e \approx p_e g W_e$ in the last term gives

$$\frac{R}{2gC_P}\left(\frac{dQ}{dt}\right)_{500} = \frac{\partial}{\partial t}\left(\bar{z}_{750} + \frac{z_{250} - 3z_{750}}{2}\right) + \mathbf{v}_{750}\cdot\nabla(\bar{z}_{750} + G - z_{1000}) + + \frac{P^\star\sigma_{500}\,\varrho_{1000}\,W_{1000}}{2} \tag{10}$$

where W is the vertical velocity, $\frac{dz}{dt}$. At 1000 mbs, $W_{1000} \approx \mathbf{v}_{1000}\cdot\nabla S$ where S denotes the contours of topography.

Equations (10) can be written

$$\frac{R}{2gC_P}\left(\frac{dQ}{dt}\right)_{500} = \frac{\partial}{\partial t}\left(\bar{z}_{750} + \frac{z_{250} - 3z_{750}}{2}\right) + \mathbf{v}_{750}\cdot\nabla(\bar{z}_{750} + G - z_{1000}) + + \frac{P^\star\sigma_{500}\varrho_{1000}}{2}(\mathbf{v}_{1000}\cdot\nabla S) \tag{11}$$

Converting the advective terms to finite difference Jacobians where a distance increment of $d = 1000$ kilometers is used, gives

$$\left(\frac{dQ}{dt}\right)_{500} \approx$$
$$\approx 6\times 10^{-6}\left[\left(\bar{z}_{750} + \frac{z_{250} - 3z_{750}}{2}\right)_{24} - - \left(\bar{z}_{750} + \frac{z_{250} - 3z_{750}}{2}\right)_0\right] +$$
$$+ 4\times 10^{-7}[(z_{750})_1 - (z_{750})_3]\cdot$$
$$\cdot[(\bar{z}_{750} + G - z_{1000})_2 - (\bar{z}_{750} + G - z_{1000})_4] -$$
$$- 4\times 10^{-7}[(z_{750})_2 - (z_{750})_4]\cdot$$
$$\cdot[(\bar{z}_{750} + G - z_{1000})_1 - (\bar{z}_{750} + G - z_{1000})]_3 +$$
$$+ 2.5\times 10^{-8}[(z_{1000})_1 - (z_{1000})_3][S_2 - S_4] -$$
$$- 2.5\times 10^{-8}[(z_{1000})_2 - (z_{1000})_4][S_1 - S_3] \tag{12}$$

cal gm^{-1} sec^{-1}.

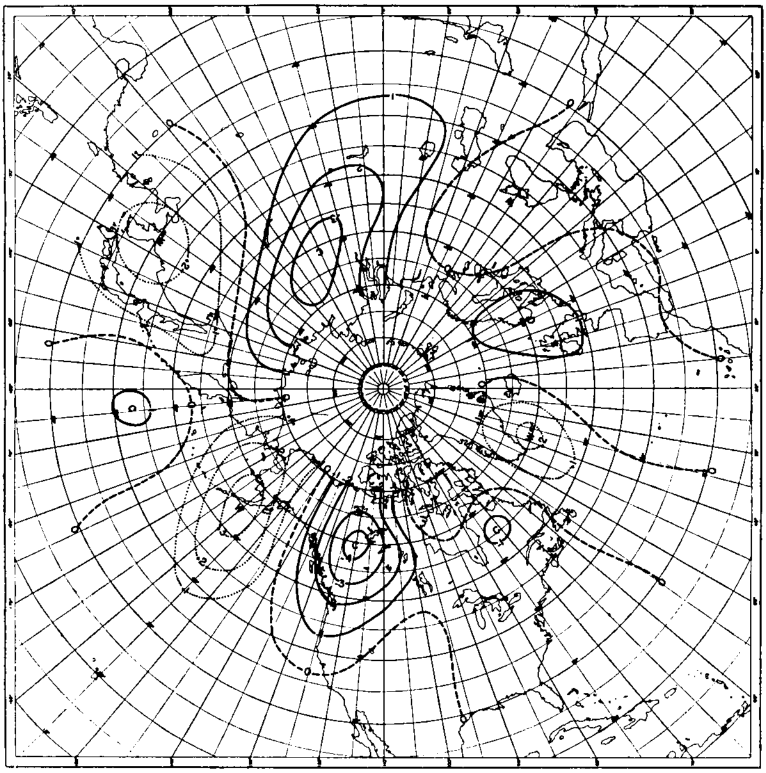

Fig. 9. Hemispheric distribution of heat-sources and heat-sinks for December 15—30, 1957. Isolines are drawn for units of 4×10^{-6} cal gm^{-1} sec^{-1}.

Intervals of 100 feet are used in reading the height values to compute the Jacobians, and in expressing the "instantaneous" tendency about the intial time, t_0. This tendency is obtained from 24-hour height changes centered about the intervening 500-mb analysis.

The evaluation of (12) involves the calculation of a height change and two Jacobians. One of the Jacobians, however, needs to be evaluated only for regions of sloping terrain.

The 750 height is computed graphically as the average of

$$z_{500} \text{ and } z_{1000}$$

A space mean of this height gives $\bar{z}$ 750. The first Jacobian in (12) is computed by orienting one axis of a plastic grid along a 750-mb contour thus causing one term in the calculation of this Jacobian to become zero. The second Jacobian is computed by orienting one of the grid axis along lines of constant S thereby causing one of the terms in this Jacobian also to become zero. Such procedures, in addition to facilitating the computation, minimize the chance for error in estimating values from a contour analysis.

The average heights above sea level of the earth's topography were obtained using sectors of 5 deg. longitude and 5 deg. latitude. Contours of these values in hundreds of feet are used for S in equation 12.

One of the major errors in obtaining $\frac{dQ}{dt}$ in equation 12 arises from the estimation of "instantaneous" tendency from maps spaced 12 hours apart. In an effort to minimize this source of error, the terms in equation 12 were computed every twelve hours. These values were then averaged over five and fifteen day periods.

The local changes tend to zero everywhere on such an average. However, there are some places where the values of the Jacobians are not randomly distributed and *do not* average to zero. In such places the magnitudes of the averaged Jacobian are sufficiently large, compared to the averaged tendencies, that errors resulting from inaccurately estimated instantaneous tendencies assume a very minor role.

A hemispheric map illustrating the average distribution of $\frac{dQ}{dt}$ for December 15—30, 1957, is presented in figure 9. The term involving the Jacobian of the terrain has not been included in this figure. Fig. 9 shows the largest "heat sources" near Korea, the Gulf of Alaska and the coastal waters east of Greenland. The major "cold" sources are found over Siberia, Northwest Canada and Scandinavia. To assess the strength of these fields in other terms, the average temperature change associated with the non-adiabatic warming near Korea would amount to between $3^1/_2$ and 4° centigrade per 24 hours.

Variations in the magnitude of $\frac{dQ}{dt}$ are closely related to changes in the flow patterns. As an illustration, differences in the 5-day mean 750 mb contour patterns between the periods December 26—30 and December 21—25, 1957 are superimposed as solid lines in fig. 10 upon changes of $\frac{dQ}{dt}$ (obtained by averaging the Jacobians over the same two periods and subtracting). The letters "INC" refer to a higher average value of $\frac{dQ}{dt}$ for December 26—30 than for December 21—25. The term "DEC" has the opposite connotation. In figure 10 the centers of increased $\frac{dQ}{dt}$ are, in general, located in advance of the positive 750-mb contour-change centers. Similarly the regions labeled "DEC" lead the centers of negative changes in the height contours.

Note, in particular, the region over Central Asia where the observed 750-mb heights averaged approximately 1000 feet higher during December 26—30 than during December 21—25, 1957. This is also a region normally considered as being a major cold source (see figure 9). To the east of an abnormally strong upper level ridge, established in conjuction with the aforementioned height rises, the normally persistent "cold source" was observed to weaken considerably as evidenced by the changes in $\frac{dQ}{dt}$ in figure 10. This change in "non-adiabatic" heating was apparently associated with the increased northerly wind components aloft which advected *even colder air* into this region, thereby, in essence, changing the region, normally considered a "cold source", into a "heat source". Other areas where large changes in "non-adiabatic" heating are observed to accompany changes in upper level circulation have been discussed by various authors, for instance, WINSTON (1955).

These observations of the close association between heating and wind direction suggest that (although improvement in the model might be obtained by considering geographically fixed or seasonally averaged "heat" and "cold" sources) some attempt should be made to introduce a heating function into the model which is free to change with the circulation pattern. If it is not found feasible to incorporate such a function directly into the forecast equations, perhaps an empirical approach would be feasible.

Purely speculating on this latter approach, since it has been found that some of the largest forecast errors are associated with wave number 1 which is, in turn, related to the "eccentricity" of the circumpolar vortex; (LASEUR, 1954) perhaps an analysis or device which eliminates this eccentricity would minimize the large scale forecast errors. Alternately, assuming it can be shown that the "eccentricity" provides an index to the existing large scale patterns of "non-adiabatic" heating, perhaps empirically determined heating functions (based on data selected for a few well-marked, and widely-different, eccentricity patterns) could be computed and stored in the machine. Changes in the heating function could then presumably be made during the forecast by having the machine compute the eccentricity at various stages. Such procedures might conceivably provide an empirical mean of incorporating a varying heating function into extended period forecasting.

Currently, relationships between changes in $\frac{dQ}{dt}$ and changes in the 24-, 48-, and 72-hour forecast error fields are being investigated. If a relationship exists, it is not readily apparent from a preliminary inspection. However, it is

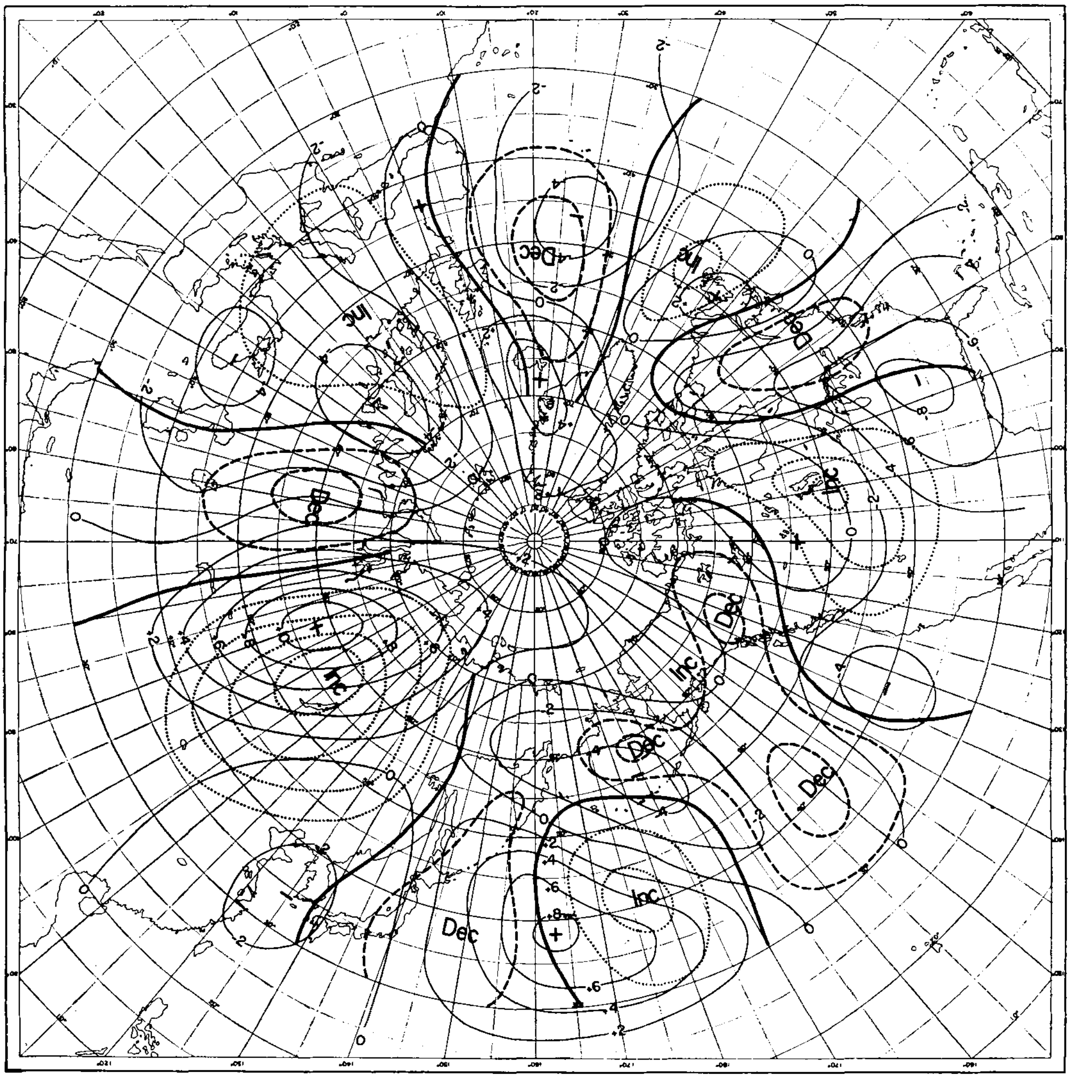

Fig. 10. A comparison between changes in circulation and changes in "non-adiabatic" heating. Solid lines show the difference in hundred of feet between the mean 750 mb contours for December 21—25, and December 26—30, 1957. The dashed and dotted isolines denote the averaged change of $\left(\frac{dQ}{dt}\right)$ in units of 4×10^{-6} cal gm^{-1} sec^{-1} between these same 5-day periods.

believed that a study of the non-adiabatically-produced divergence and vertical motion fields will throw additional light on this relationship.

Acknowledgements

The author wishes to express his sincere thanks to Dr Bert Bolin who suggested the initiation of this study and whose many helpful ideas offered constant direction and encouragement throughout the course of investigation.

It is also a pleasure to acknowledge Fil. lic. Aksel Wiin-Nielsen who provided a constant source of help and information. Mr. Nielsen's efforts were particularly instrumental in helping

to devise the model for computing the "non-adiabatic" effects discussed in section V.

Appreciation is expressed to JNWPU and NWAC for supplying the basic data used in this investigation.

The able assistance of Miss Berit Jacobsson in performing many of the computations presented in this report is grateful acknowledged.

Gratitude is also extended to Captain Russel G. Harris and Mr. Leonard Snellman of Scientific Services, Air Weather Services, for reading the manuscript and offering many helpful editorial suggestions.

REFERENCES

BOLIN, B., 1955: Numerical forecasting with the barotropic model. *Tellus* **7**, pp. 27—49.

FJØRTOFT, R., 1952: On a numerical method of integrating the barotropic vorticity equation. *Tellus*, **4**, pp. 179—194.

HARRIS, R. G., 1956: The application of harmonic analysis procedure to routine forecasting. (Unpublished).

LASEUR, N. E., 1954: On the asymmetry of the middle-latitude circumpolar vortex. *Journal of Met.* **11**, pp. 43—57.

MARTIN, D. E., 1956: Forecasting rules and techniques used in Tokyo Weather Central. IWW special study 105-2, p. 104.

SIGTRYGGSSON, H., and WIIN-NIELSEN, A., 1957: Experiments in numerical forecasting using space-smoothing fields. *Tellus*, **9**, pp. 296—312.

WHITE, R. M., and COOLEY, D. S., 1956: Kinetic energy spectrum of meridional motion in mid-troposphere. *Journal of Met.* **13**, pp. 67—69.

WINSTON, J. S., 1955: Physical aspects of rapid cyclogenesis in the Gulf of Alaska. *Tellus*, **7**, pp. 481—499.

WOLFF, P. M., 1958: The errors in numerical forecasts due to retrogression of ultra-long waves. *Tech. Mem.* No. 13, JNWPU.